UCRL-TR-227795

LAWRENCE LIVERMORE NATIONAL LABORATORY

Development and Application of a Predictive Computational Tool for Short-Pulse, High-Intensity Target Interactions

R. P. J. Town, H.-K. Chung, A. B. Langdon, B. F. Lasinski, S. M. Lund, B. C. McCandless, C. H. Still, and M. Tabak.

February 6, 2007

Final Report LDRD 04-ERD-054.

Disclaimer

Auspices Statement

This work was performed under the auspices of the U. S. Department of Energy (DOE) by the University of California, Lawrence Livermore National Laboratory (LLNL) under Contract No. W-7405-Eng-48. The project 04-ERD-054 was funded by the Laboratory Directed Research and Development Program at LLNL.

Final Report LDRD 04-ERD-054

Development and Application of a Predictive Computational Tool for Short-Pulse, High-Intensity Target Interactions*

R. P. J. Town, H.-K. Chung, A. B. Langdon, B. F. Lasinski, S. M. Lund,
B. C. McCandless, C. H. Still, and M. Tabak
Lawrence Livermore National Laboratory, Livermore, CA 94551-0808, USA

Abstract

The widely differing spatial, temporal, and density scales needed to accurately model the fast ignition process and other short-pulse laser-plasma interactions leads to a computationally challenging project that is difficult to solve using a single code. This report summarizes the work performed on a three year LDRD to couple together three independent codes using PYTHON to build a new integrated computational tool. An example calculation using this new model is described.

*This work was performed under the auspices of the U. S. Department of Energy (DOE) by the University of California, Lawrence Livermore National Laboratory (LLNL) under Contract No. W-7405-Eng-48. The project 04-ERD-054 was funded by the Laboratory Directed Research and Development Program at LLNL.

Introduction

Powerful short pulse high intensity lasers enable a number of programmatically important applications that would be difficult, if not impossible, to accomplish by other means. These applications include: the exploration of the fast ignition concept[1] for inertial fusion energy (IFE); the production of very high temperature hohlraums to drive and probe opacity experiments; the production of very high-energy photon backlighters[2] to probe imploded material configurations; the generation of high energy proton beams to probe electric and magnetic fields; and the generation of very intense proton beams to heat material samples for EOS and opacity experiments, or to probe dense samples. However, we did not have a predictive integrated computational capability to model in detail the relevant physics associated with any of these proposed applications. Consequently, the goal of this LDRD project was to develop the theoretical understanding and computational capability to guide current experiments at small-scale short-pulse laser facilities, and make credible predictions about the likely performance of high-energy short-pulse laser facilities currently under construction. We achieved this goal by coupling together different existing simulation codes that had been optimized for specific spatial and temporal scales into one virtual code using the PYTHON programming language.

This paper is organized as follows. In Section I we briefly review the physical characteristics of the Fast Ignition (FI) problem, which represents probably the most challenging short-pulse laser-plasma problem that our code needs to model. Section II describes the approach that we have taken to develop the computational tool and reviews the physics packages of the three component codes. Section III describes an example calculation of a proposed Fast Ignition experiment. Finally, section IV summarizes the main results of this LDRD project. A list of publications arising from the project are detailed in appendix A.

I. Description of the Problem

Unlike the conventional hot-spot approach[3] to achieving inertial confinement fusion (ICF), the FI approach separates fuel compression from the ignition phase. A typical cone-guided FI-target geometry is shown in Figure 1. In the compression phase, the compression laser beams (or x rays generated by laser beams absorbed by a hohlraum wall) deposit their energy onto the outside of a spherical shell that rapidly heats up and ablates outwards. The ablation plasma acts like a rocket's exhaust driving the remaining shell inward compressing the fuel contained within the shell to form a uniform dense fuel assembly with a density, ρ, of ~300 g/cm^3, and an areal density $\rho R \sim 3.0$g/cm^2, where R is the radius of the fuel. This phase involves modeling capsules over millimeter spatial scales for tens of nanosecond. It is naturally modeled using radiation hydrodynamics codes that have been developed for conventional ICF research.

In order to ignite the compressed fuel assembly it is necessary to deposit tens of kilojoules into a small spot heating the fuel to ignition conditions and thus initiating a propagating burn wave. The ignition energy must be delivered in a short time compared

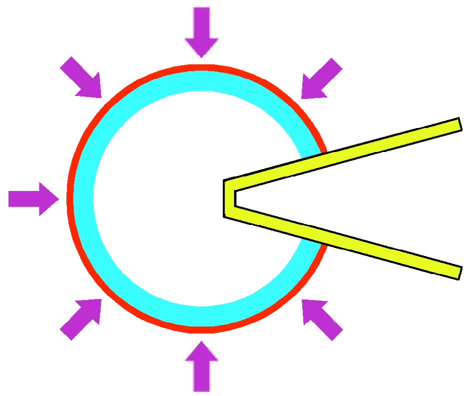

Figure 1: Typical Fast Ignition target cone-focused target geometry.

to the fuel disassembly time. For the typical compressed fuel configuration described above, the energy needs to be delivered in a ~20 μm radius spot in less than 50 ps. The ignition phase naturally breaks down into several steps that have unique physics challenges. First, the ignition laser propagates in the clear channel created by the cone to the tip of the cone, where a beam of relativistic electrons is generated. The spatial, temporal, and density scales involved in these relativistic laser-plasma interactions naturally lend this interaction to be modeled by explicit particle-in-cell (PIC) codes.

Next, the relativistic electron beam (REB) formed by the interaction of the intense laser with the plasma propagates to the dense core. The electrons travel over a large density range since they are born at the relativistic critical density (above which the laser cannot propagate) which for 1 μm light is above 1.1×10^{21} cm^{-3} and propagates up to the dense fuel, which is at ~10^{26} cm^{-3} over a distance of ~100μm. Such conditions are best modeled using hybrid implicit PIC codes, since traditional explicit PIC codes have cell sizes on order of the Debye length, which for typical conditions is of the order of 10^{-8} cm making explicit PIC codes impractical for full-scale simulations.

Finally, the relativistic electrons deposit their energy into the fuel and initiate a burn wave that propagates across the fuel. The deposition itself is best modeled by the implicit hybrid PIC code used for transport, but the burn wave propagation is most easily modeled using standard radiation hydrodynamics codes used in conventional ICF research.

A variation of FI, called proton-driven FI[4], involves the conversion of the REB into an intense beam of protons. This conversion takes place in a thin hydrogen-rich layer on the back surface of a thin foil. This process can be most readily modeled using an explicit PIC code. The subsequent transport of the proton beam is modeled using an implicit hybrid PIC code for the same reasons as described for REB transport above.

II. Method of Solution

The widely differing spatial, temporal, and density scales needed to accurately model the FI process leads to a computationally challenging project that is difficult to solve using one code employing a single solution technique. As section I described, the individual processes naturally require a radiation hydrodynamics code, an explicit PIC code, and a hybrid implicit PIC code. In addition, current and future experiments field a wealth of optical, and particle diagnostics that need to be simulated to enable quantitative

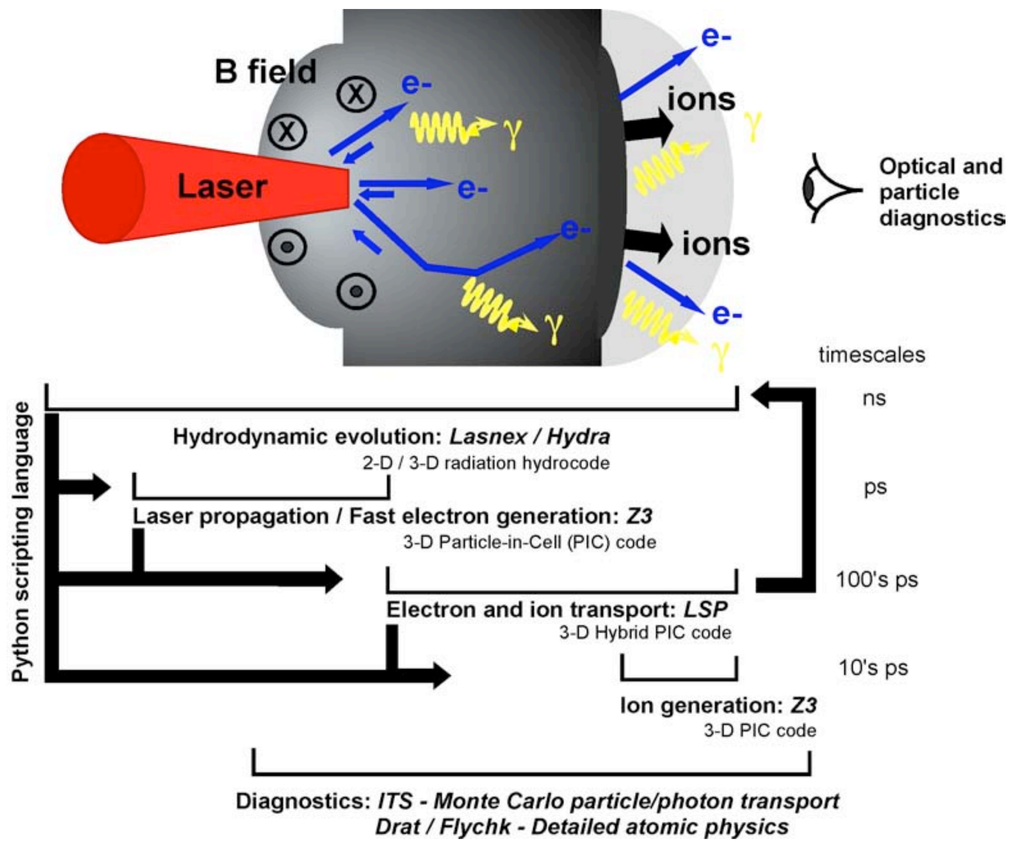

Figure 2: We use the PYTHON programming language to couple together independent physics code to form one virtual FI research tool.

comparisons between modeling and experiments. We integrated these different physics codes using the PYTHON programming language to form a virtual code. Figure 2 graphically shows the various codes that are used with their spatial and temporal scales along with the interconnections that have been implemented. Each of the individual codes is briefly reviewed below.

LASNEX: Radiation Hydrodynamic Code.

LASNEX[5] is a 2-D multi-physics radiation hydrodynamics code developed at LLNL that contains all the relevant physics to model an ICF implosion. LASNEX uses a 2-D, axially symmetric mesh composed of arbitrarily shaped quadrilaterals. The hydrodynamics is Lagrangian followed by an optional rezone step. A flux-limited Spitzer/Braginskii electron thermal transport, modified to include dense plasma effects, is used to transport electrons. Multigroup flux limited diffusion for radiation transport and a fully 3-D ray trace package for inverse bremsstrahlung laser energy deposition is included. LASNEX calculates all significant thermonuclear reactions. The atomic physics models, such as QEOS[6], in LASNEX supply the equation-of-state variables used in the hydrodynamics, the ionization state, and the frequency dependent opacities.

The time-dependent output of the LASNEX calculations is stored in portable database system[7] (PDB) files, which can be read by our PYTHON scripts to translate the distorted LASNEX mesh to a fixed orthogonal mesh for use by the explicit PIC code, Z3, and the implicit hybrid PIC code, LSP. Typically this is performed to establish the plasma conditions around peak compression for the transport phase for use with LSP and to establish the plasma condition wrought by the pre-pulse for the short-pulse laser for use with Z3.

Z3: Explicit Particle-in-Cell Code.

Z3 is a 3-D massively parallel relativistic explicit PIC code developed at LLNL under a previous LDRD project[8]. Z3, and its predecessor, ZOHAR, have been used for modeling laser-plasma interactions at moderate to high intensities for many years. On present parallel computers Z3, in 2D, can readily model laser propagation in systems up to 100 μm x 100 μm (comparable to the short pulse laser spot) with peak density well above the relativistic critical density with full collisionless physics.

Like LASNEX, Z3 stores the time-dependent output in PDB files, which can be read by our PYTHON scripts to extract the relativistic electron distribution to be used by LSP to transport the electrons through a dense cold plasma.

LSP: Hybrid Implicit Particle-in-Cell Code.

LSP[9] is a fully 3-D hybrid PIC code capable of running in Cartesian, cylindrical, or spherical geometry that was developed at Mission Research Corporation for use in the ion beam community. It employs a relativistic direct implicit particle push based on the algorithm developed by Friedman et al[10] and Hewett and Langdon[11]. LSP incorporates inter- and intra-species collisions based on Spitzer collision frequencies. Electrons can dynamically switch between kinetic and fluid treatments, depending on the ratio of their kinetic energy to the local fluid thermal energy. In the fluid description the electrons carry a temperature, which is advanced by a separate energy equation that greatly reduces the effect of numerical cooling. During the LDRD project, we added a more realistic QEOS model. The original Spitzer conductivity was enhanced by the recent addition of a Lee-More model[12] for electron conductivity. The code has a module based on the ITS code[13] to calculate line radiation and bremsstrahlung produced by energetic electrons. LSP uses the MPI library for parallelization, and has a dynamic load-balancing algorithm.

We have made substantial modifications to LSP in order to better integrate it with the other components of the project. In particular, the control parameters set and problem generator has been described in PYTHON. The ability to read and write PDB files has also been added to facilitate data exchange between codes. This has allowed far more complicated problems to be initialized, including the ability to read the LASNEX-generated plasma conditions and the Z3-produced hot electron distributions. The time-loop was exposed to PYTHON, which has enabled the code to be controlled as the simulation progresses. In order to more directly compare with the experimental

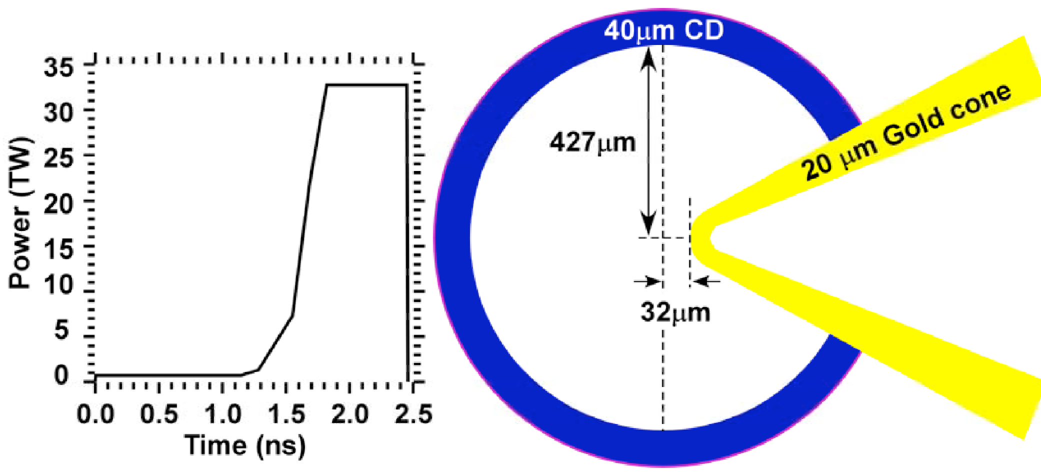

Figure 3: The target geometry and laser pulse history for a non-cryogenic OMEGA-EP cone focused implosion experiment.

observations the radiation model was upgraded from the original cold cross-sections to include thermal effects in the atomic line positions and fluorescence yields[14].

III. An Integrated Fast Ignition Simulation

As an example of our enhanced code capability we report on simulations of a proposed subscale FI experiment that will be performed at the OMEGA-EP short-pulse laser facility, which is currently under construction at the University of Rochester's Laboratory for Laser Energetics. There is a large parameter space to explore for cone-guided FI experiments using either direct- or indirect-drive[15]. For this review, the capsule consists of an empty 40 µm thick CD shell at a radius of 427 µm. Inserted into the side of the capsule is a 35° 20 µm thick gold cone, whose tip is offset from the center by 32 µm. The capsule is directly driven by a 55 beams of the OMEGA laser's 60 beams by a shaped laser pulse that consists of a 1-ns low intensity foot rising smoothly to a peak of 33TW (see Figure 3). The radiation hydrocode portion of our computational tool (LASNEX) simulates the implosion through to around peak compression. The density and temperature profiles are then passed through our PYTHON scripts to LSP for the relativistic electron transport calculation part of the problem. Figure 4 shows these profiles along with the position of the gold cone tip (shown with a yellow line) and the core size (shown with a black line) used to normalize the spatial scale. In the process of forming the dense fuel the gold cone has been severely distorted and pushed

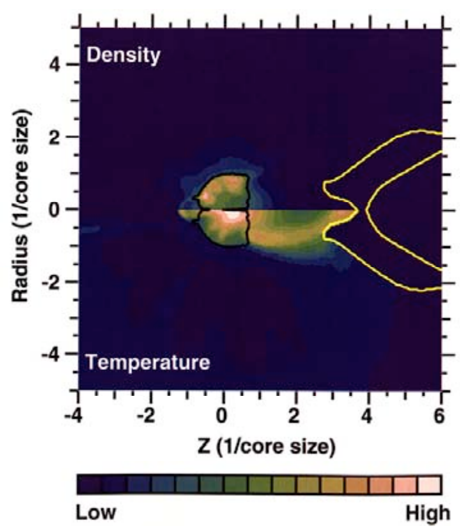

Figure 4: The background plasma density and temperature profiles at around peak

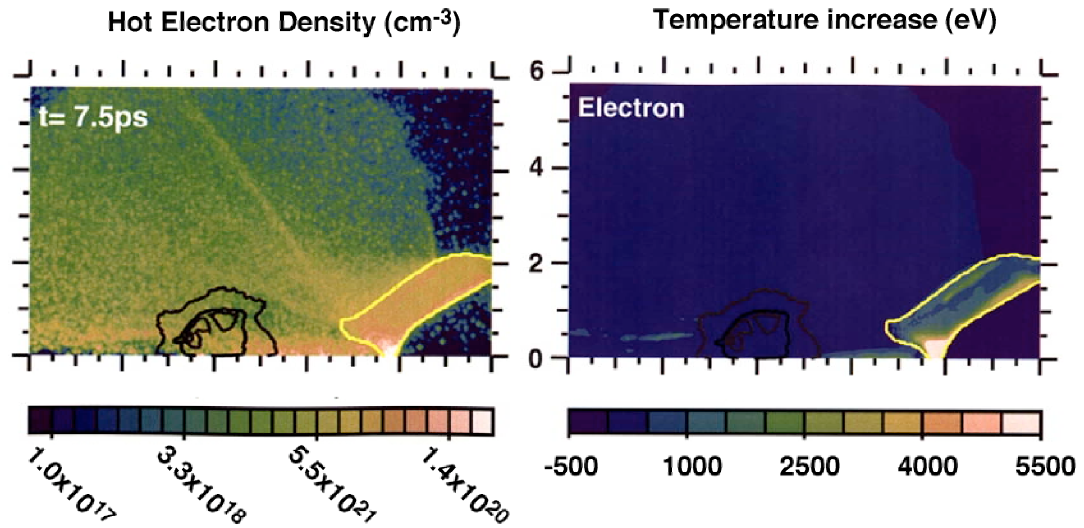

Figure 5: The relativistic electron density at 7.5 ps. The increase in background plasma electron temperature at 10 ps.

back such that the distance between the short-pulse laser side of the gold cone and the dense fuel is about 4 core-radii. In order to determine the birth energy of the relativistic electrons, we assumed that the OMEGA-EP short pulse laser will deliver 1-kJ of energy into a 20 μm laser spot in a 5 ps square-top pulse. This laser pulse generates about 150J of relativistic electrons with a peak energy of 4 MeV in the central portion of beam falling to less that 500 keV in the wings of the laser spot.

Figure 5 shows the relativistic electron density distribution at 7.5-ps. The hot electrons are born along the right hand edge of the gold cone. Most of the electrons are confined to the gold cone (shown with a yellow line in the figure). Those that escape the cone travel toward the dense fuel region, although a significant number do not make it to the high-density region. The right hand plot of Figure 5 shows the temperature increase of the background plasma electrons. The majority of the relativistic electron energy has been deposited into the cone and only a small temperature increase is seen in the fuel.

These results demonstrate the integrated capability of the LDRD-funded computational tool, which is now being applied to optimize FI designs. We are, for example, using a short-pulse laser pulse that contains more energy in a smaller focal spot that is closer to OMEGA-EP's design specification. This leads to a higher intensity on target that generates higher energy electrons. We are also working to minimize the gold cone thickness through which the relativistic electrons must pass.

IV. Summary

Over the three-year LDRD grant, we have developed an integrated computational model that we have begun to apply to short-pulse laser-plasma interaction studies, such as cone-focused FI experiments. The newly developed tool uses PYTHON to couple together existing codes that have been developed over a number of years to model particular aspects of FI. Of the three codes used in this project the implicit hybrid PIC code, LSP, has seen the most development with the addition of a PYTHON interface and new physics models.

The success of this project has led to a further funded LDRD on using the computational tool to develop short-pulse laser applications. Our modeling capability has also been applied to guide experimental design and interpretation of experimental data in a number of short-pulse laser-plasma projects at LLNL.

The computational tool has become the standard tool for modeling short-pulse laser-matter interactions not only at LLNL, but also at the University of Rochester's Laboratory for Laser Energetics, and the Ohio State University. The LSP code vendor is adopting the changes that we have made for future release to the community.

A. Publications Resulting From This LDRD

1. H.-K. Chung, M. H. Chen, and R. W. Lee, *"Extension of Atomic Configuration Sets of the Non-LTE Model in the Application to the Kα Diagnostics of Hot Dense Matter"*, submitted to High Energy Density Physics (2006). UCRL-JRNL-226606
2. M. Tabak, D. Hinkel, S. Atzeni, E. M. Campbell, and K. A. Tanaka, *"Fast Ignition: Overview and Background"*, Fusion Science and Technology **49**, 254 (2006). UCRL-JRNL-213396
3. C. K. Li, F. H. Seguin, J. R. Rygg, R. D. Petrasso, R. P. J. Town, P. A. Amendt, S. P. Hatchett, O. L. Landen, A. J. Mackinnon, P. K. Patel, V. A. Smalyuk, T. C. Sangster, and J. P. Knauer, *"Measuring E and B Fields in Laser-Produced Plasmas with Monoenergetic Protons Radiography"*, Phys. Rev. Lett. **97**, 135003 (2006). UCRL-JRNL-220964
4. C. K. Li, F. H. Seguin, J. R. Rygg, R. D. Petrasso, R. P. J. Town, P. A. Amendt, S. P. Hatchett, O. L. Landen, A. J. Mackinnon, P. K. Patel, V. A. Smalyuk, T. C. Sangster, and J. P. Knauer, *"A Monoenergetic Proton Backlighter for Measuring E and B Fields and for Radiographing Implosions and HED Plasmas"*, Rev. Sci. Instrum **77**, 10E725 (2006). UCRL-JRNL-221036
5. S. Atzeni, and M. Tabak, *"Overview of Ignition Conditions and Gain Curves for the Fast Ignitor"*, Plasma Phys. Control. Fusion, **47**, B769 (2005). UCRL-JRNL-213654
6. R. P. J. Town, C. Chen, L. A. Cottrill, M. H. Key, W. L. Kruer, A. B. Langdon, B. F. Lasinski, R. A. Snavely, C. H. Still, M. Tabak, S. C. Wilks, and D. R. Welch, *"Simulations Of Electron Transport For Fast Ignition Using LSP"*, Nucl. Inst. Meth. Phys. Res. A, **544**, 61 (2005). UCRL-PROC-204414
7. J. A. King, K. Akli, R. A. Snavely, B. Zhang, M. H. Key, C. D. Chen, M. Chen, S. P. Hatchett, J. A. Koch, A. J. Mackinnon, P. K. Patel, T. Phillips, R. P. J. Town, R. R. Freeman, M. Borghesi, L. Romagnani, M. Zepf, T. Cowan, R. Stephens, K. Lancaster, C. Murphy, P. Norreys, and C. Stoeckl, *"Characterization of a picosecond laser generated 4.5 keV Ti K-alpha source for pulsed radiography"*, Rev. Sci. Instrum. **76**, 76102 (2005). UCRL-JRNL-210865
8. M. Tabak, D. S. Clark, S. P. Hatchett, M. H. Key, B. F. Lasinski, R. A. Snavely, S. C. Wilks, R. P. J. Town, R. Stephens, E. M. Campbell, R. Kodama, K. Mima,

T. A. Tanaka, S. Atzeni, and R. R. Freeman, *"Review of progress in fast ignition"*, Phys. Plasma **12**, 57305 (2005). UCRL-CONF-207839

9. J. A. King, K. Akli, B. Zhang, R. R. Freeman, M. H. Key, C. D. Chen, S. P. Hatchett, J. A. Koch, A. J. MacKinnon, P. K. Patel, R. A. Snavely, R. P. J. Town, M. Borghesi, L. Romagnani, M. Zepf, T. Cowan, H. Habara, R. Kodama, Y. Toyama, S. Karsch, K. Lancaster, C. Murphy, P. Norreys, R. Stephens, and C. Stoeckl, *"Ti K Alpha Radiography of Cu-Doped Plastic Microshell Implosions Via Spherically Bent Crystal Imaging",* Applied Physics Letters **86**, 191501 (2005). UCRL-JRNL-210564
10. M. Tabak, and D. A. Callahan, *"Models of Gain Curves for Fast Ignition",* Nucl. Inst. Meth. Phys. Res. A, **544**, 48 (2005). UCRL-CONF-204393
11. A. J. Mackinnon, P. K. Patel, R. P. J. Town, M. J. Edwards, T. Phillips, S. C. Lerner, D. W. Price, M. H. Key, S. Hatchett, S. C. Wilks, M. Borghese, L. Romagnani, S. Kar, T. Toncian, G. Pretzler, O. Willi, M. Koenig, E. Martinolli, S. Le Pape, A. Benuzzi-Mounaix, P. Audebert, J. C. Gauthier, J. King, R. Snavely, R. R. Freeman, T. R. Boehly, *"Proton Radiography as an Electromagnetic field and Density Perturbation Diagnostic"*, Rev. Sci. Instrum **75**, 3531 (2004). UCRL-CONF-203614

References

[1] M. Tabak, *et al.*, Physics of Plasmas **1**,1626 (1994).
[2] K. B. Wharton, *et al.,* Phys. Rev. Lett. **81,** 822 (1998).
[3] J. D. Lindl, *Inertial Confinement Fusion. The Quest for Ignition and Energy Gain Using Indirect Drive* (Springer, New York, 1998).
[4] M. Roth, *et al.*, Phys. Rev. Lett. **86**, 436 (2001).
[5] G. B. Zimmerman, and W. L. Kruer, Comment Plasma Phys. Contr. Fusion 2, **85** (1975).
[6] R. M. More, K. H. Warren, D. A. Young, and G. B. Zimmerman, Phys. Fluids **31**, 3059 (1988).
[7] S. A. Brown, and D. Braddy, "PACT Users' Guide," Lawrence Livermore National Laboratory, Livermore, CA, UCRL-MA-112087 (1995).
[8] A. B. Langdon and B. F. Lasinski, in *Methods in Computational Physics*, ed. by B. Alder and S. Fernbach, vol. ed J. Killeen, (Academic Press, New York), Vol. 16, 1976; and C. K. Birdsall and A. B. Langdon, *Plasma Physics via Computer Simulation* (McGraw-Hill, New York, 1985).
[9] D. R. Welch, D. V. Rose, B. V. Oliver, and R. E. Clark, Nucl. Inst. Meth. Phys. Res. A **464**, 134 (2001).
[10] A. Friedman, A. B. Langdon, B.I. Cohen, Comment Plasma Phys. Contr. Fusion **6**, 225 (1981).
[11] D. W. Hewett, and A. B. Langdon, J. Comp. Phys. **72**, 121 (1987).
[12] Y. T. Lee, and R. M. More, Phys. Fluids **27**, 1273 (1984).
[13] J. A. Halbleib, *et al.*, IEEE Trans. Nucl. Sci. **NS-39**, 1025 (1992).
[14] H.-K. Chung, *et al.*, High Energy Density Physics **1**, 3 (2005).
[15] S. P. Hatchett, *et al.,* Fusion Science and Technology **49**, 327 (2006).